On the Reliability of the Fractal Dimension as a Scalar Characteristic of the Medical Images' Contours

ELENA HADZIEVA*[1], DIJANA C. BOGATINOSKA[1], MARIJA SHUMINOSKA[1], RISTO PETROSKI[1]
[1]University of Information Science and Technology "St. Paul the Apostle"
Partizanska bb, 6000 Ohrid
FORMER YUGOSLAV REPUBLIC OF MACEDONIA
{elena.hadzieva, dijana.c.bogatinoska}@uist.edu.mk, {marija.shuminoska, risto.petroski}@cse.uist.edu.mk

Abstract: - Medical images typically have irregular and fragmented contours. This is a strong motivation to use fractal geometry, rather than Euclidian geometry, for their description and characterization. In this paper we analyse a set of 100 images of melanoma and non-melanoma moles. The moles have their contours extracted with several tools and then the contours have their fractal dimension computed with distinct estimators. We have used descriptive statistics to depict that the fractal dimension does not give clear classification or systematization of the moles. We have also applied the student's *t*-test to show that in the considered cases the two sets of fractal dimensions of melanoma and non-melanoma moles are not statistically different.

Key-Words: - moles, contours, medical diagnosing, fractal dimension, reliability, student's *t*-tests.

1 Introduction

Fractal analysis is a mathematical field that deals with fractal characteristics of data. Its most important parameter is the fractal dimension, which will be defined and discussed later in this paper. The fractal dimension is considered to be a measure of the complexity, or irregularity, of a fractal object. Medical images are objects with typical fractal, non-Euclidean, structure - the fact that led the scientific community to apply the tools of fractal analysis in medical diagnosing. The visual difference in smoothness between normal and abnormal tissues (or cells) has motivated the use of fractal dimension as a diagnosing tool: the first supposed to have lower complexity, i.e. lower fractal dimension, whilst the latter supposed to have higher complexity, i.e. higher fractal dimension.

We have tried to reproduce closely the results met in several papers for successful application of fractal dimension for description and classification of tissues with and without cancer ([1-7]). We have targeted skin cancer, taking into consideration the previously reported results ([1], [4-7]) and the famous dermatological *ABCDE* rule. In summary, the rule describes the warning signs for melanoma ([23]): *A* stands for asymmetrical form (melanoma moles are often asymmetrical); *B* stands for border (melanoma moles typically have irregular border); *C* stands for colour (when more than one colour or different shades from one colour are present, the mole is considered to be suspicious); *D* stands for diameter (diameter of melanoma moles is usually greater than 6mm); *E* stands for evolution (how the previously normal mole is evolving, i.e. changing its colour and shape). Taking into account the *B* indicator, and, as already mentioned, previous results, we were expecting, at least in statistical sense, higher fractal dimension of melanoma moles' contour lines. Unfortunately, all our efforts to reproduce the results from the papers, were unsuccessful, i.e. they were not giving neither expected results, nor any systematization or differentiation of melanoma and non-melanoma moles. Thus, we came to the challenging question: is the fractal dimension reliable or not to be used as a tool in medical diagnosing? Our investigations showed that it is not reliable parameter.

The paper continues as follows. Section 2 resumes some published results related to the topic. In Section 3 we give few mostly used definitions of fractal dimension and related discussion. In the next section, Data and Methods, we give a description of data and methods used for this research. This section is followed by Results and Discussion and Conclusion sections.

2 Related work

The authors in [6] compare the detection rate of malignant melanoma based on clinical visual investigation of about 65% with their approach based on fractal analysis, which gives significant 79.1% correctness. Moreover, the approach of Klein et al. in [2] gives high 97% of correctness in identifying malignant cells, which sounds remarkable compared to the current best tumor marker for pancreatic adenocarcinoma CA19-9 - it has its own sensitivity of 50 - 70% and applied jointly with two other tumor markers, the sensitivity is up to 85%. Dobrescu et al. in [7] claim that fractal and texture analyses can discriminate between the shapes of benign and malignant tumors. Fractal analysis and geometry have many applications other than diagnosing cancer. Indeed, they have application in image analysis in general, and especially in the medical fields (classifying ECG and EEG signals, brain, mammography, bone images, see for example the review given in [8]). All of these papers use the fractal dimension, computed with different methods, as one of the factors for classification and diagnosing.

On the other hand, there are papers that report the non-reliability of the fractal dimension. Most of the fractal dimension estimators use the easy-to-implement box-counting method, for which the following drawbacks were recorded: binarization of the signal, construction of empty boxes, grid effect ([8]). Parameters tuning could improve the estimations by the box-counting method. But it will be not clear whether the obtained differences in fractal dimensions are results of true differences in the images or results of certain "good" decisions made during the estimation process. In the same paper ([8]), the authors conclude that no comparative analysis was done (according to our knowledge, this is still the case), which could produce the most suitable method and improvements of the existing results. The authors in [9] claim that the fractal dimension estimates depend on the estimator employed, the pixelization and resolution of the images and the structure identification technique used, and they kindly suggest that the previously reported results need revision. The authors of [10] come to a conclusion that the fractal dimension depends on the edge detection algorithm used, in the sense that thicker line yields to higher dimensional values. Other authors (see [11]) treat the inconsistency of the fractal characteristics of medical images over large scale-ranges, proving that the fractal dimension of the contours depends on the scale at which the object of interest is considered. Also, they propose a method for determining a scale or scale interval in which fractal dimension of observed tissue will have relevance in diagnosing (particularly, they work with breast cancer images, but their approach has wider application). It is known that medical images are "no reference model", i.e. they suffer from noise, that can not be objectively detected or measured. Reiss et al. in [12] found that the noise has significant effect on few commonly applied methods for computing the fractal dimension.

All of the authors cited in the last paragraph note different advantages and disadvantages in the process of calculating the fractal dimension, which they propose to be taken into consideration in order to avoid misreading of the results.

3 Theoretical grounds

When we think of fractals, we mainly think on "broken, irregular, complex, fragmented, grainy, ramified, strange, tangled and wrinkled shapes" ([13]), such as clouds, coastlines, edgy rocks, bushes, river basins, blood vessels, or lungs are. The theoretical definition of fractals can be met in many forms, but it seems like their most valid definition is the one stated by Falconer in [14]: We refer to the subset of $\mathbb{R}^n$ as a fractal if it has a fine structure, noticed even on arbitrarily small scales; it is too irregular to be described in traditional geometric language, both locally and globally; it often has some form of self-similarity, rigorous or approximate; its "fractal dimension" (defined in some way) is greater than its topological dimension; in most of the cases, it is defined in a very simple way, perhaps recursively.

As mentioned before, there are many ways to define fractal dimension. The following are the mostly used.

Definition 1 ([14], p. 29) *Let* $A \subset \mathbb{R}^m$. *The number*

$$D_H(A) = \inf\{s|\mathcal{H}^s(A) = 0\} = \sup\{s|\mathcal{H}^s(A) = \infty\},$$

where $\mathcal{H}^s(A) = \lim_{\delta\to 0} \mathcal{H}^s_\delta(A)$, $\mathcal{H}^s_\delta(A) = \inf\{\sum_{i=1}^{\infty}(\text{diam } U_i)^s : U_i \text{ is a } \delta - cover\ of\ A\}$, *is called the Hausdorff dimension (or Hausdorff-Besicovitch dimension) of the set A.*

The Hausdorff dimension satisfies the desirable properties of a dimension, from theoretical point of view: monotonicity, stability, countable stability, geometric invariance, Lipschitz invariance, countable sets, open sets and smooth manifolds properties ([15]). However, from practical point of view, it is usually avoided, due to the computational difficulties for finding its value. The next definition, although less satisfactory from

theoretical point of view, it is very popular because it is much easier for understanding and for embedding in a software tool for fractal dimension estimation.

Definition 2 ([15], p. 174) *Let* $A \in \mathcal{H}(\mathbb{R}^m)$ *and let* $N(A, \varepsilon)$ *denote the smallest number of closed balls of radius* $\varepsilon > 0$ *needed to cover the set A. If*

$$D(A) = \lim_{\varepsilon \to 0} \frac{\ln(N(A, \varepsilon))}{\ln(1/\varepsilon)}$$

exists, then $D(A)$ *is called the fractal dimension of A.*

When the existence of the fractal dimension is ensured, it can be obtained if instead of balls, boxes of side length $\varepsilon_i = \frac{1}{2^i}$, $i \in \mathbb{N}$, are used. In such case, the fractal dimension is commonly called *box-counting fractal dimension* and it can be obtained by the formula

$$D(A) = \lim_{n \to \infty} \frac{\ln(N(A, n))}{\ln 2^n}, \qquad (1)$$

where $(N(A, n))$ is the number of boxes with side-length $1/2^n$ that have nonempty intersection with A. Due to the limitation of the box-size with the size of the pixel, in practice, the fractal dimension is obtained when finite number of points $(\ln 2^i, \ln N(A, i))$ are fitted with a line, whose slope is then taken as approximation of the fractal dimension. This computational method is commonly known as basic box-counting method for the computation of the fractal dimension and it is mostly embedded in the software tools that estimate the fractal dimension.

For some theoretical fractals, it can be shown that the Hausdorff and box-counting dimensions have the same value ([15]), and in such cases they can be jointly used for obtaining powerful effect. We note that throughout the papers there is substantial inconsistency in terminology related to the different types of dimensions and algorithms used for their computation.

4 Data and methods

We have recently analyzed more than 10 software tools used for computing the box-counting fractal dimension, applying them on some theoretical fractals and we have found that five best are (see [16, 17]): Harfa ([18, 25]), FracLac ([26]), Fractalyse ([27]), Fractal Count ([28]), and Fractal Analysis System ([29]). All of the tools are freely available (the last is available upon request), and all of them use the basic box-counting method or its variations. We tested them on artificial fractals in order to configure and standardize the tools for further application. Then we considered a set of 100 biomedical images of melanoma and non-melanoma moles, obtained with the kind allowance of the first author of [19]-[22]. The images (out of which 30 are invasive malignant melanoma and 70 benign) are obtained from the EDRA Interactive Atlas of Dermoscopy and the dermatology practices of Dr. Ashfaq Marghoob (New York, NY), Dr. Harold Rabinovitz (Plantation, FL), and Dr. Scott Menzies (Sydney, Australia). These are 24-bit RGB color images with dimensions ranging from 577 × 391 pixels to 2556 × 1693 pixels.

The process of extracting the edge of the moles was mainly consisted of two parts:

1. Applying a thresholding algorithm which results in a black and white image, where the region of interest (the mole itself) is black, on a white background (the normal skin),
2. Cropping the pixels positioned on the edge between the black and white parts.

ImageJ as a suitable, widely used tool for manipulating images, has proven to be useful in our research as well. By default, ImageJ offers 17 thresholding algorithms. To make sure they are all given a chance in a reasonable effort, an ImageJ Macro script was written and put in use (available on https://gist.github.com/9bdd6a6a2fb9fbef459d). These are the steps that were automatized:

- Open the mole image;
- Conversion to 8bit (gray-scale);
- Select and apply thresholding algorithm;
- Invert colors;
- Manual selection of the region of interest using Wand Tool;
- Run the Outline tool to get the area of interest outline;
- Finally, save the result for further calculation of the fractal dimension.

After this process was completed, we obtained 1700 = 17 × 100 one pixel wide edges ready for the calculation of the fractal dimension. By visual observation, we have discriminated 400 = 4 × 100 contour-lines appropriate for further investigation, obtained by the four ImageJ thresholding algorithms: Default, Huang, Intermodes and Minimum.

Additionally, for extracting the contour-lines we used more or less standard software written in MATLAB, which also produced one pixel wide contour-lines. Here, the adjustment of the threshold parameter can be done distinctively for each image. We were trying to be as consistent as possible in the choices of this parameter, aiming to extract the whole part of the mole which is not a normal skin.

5 Results and discussion

As said in the introduction, we were expecting to obtain the results which will discriminate between the melanoma and non-melanoma moles and later to choose the thresholding algorithm and the software tool for estimating fractal dimension which will give the best differentiation. Examples of the contours obtained from the four chosen ImageJ algorithms and our MATLAB algorithm are presented on Figures 2-6 and 8-12. These are contours of a randomly chosen non-melanoma mole and a randomly chosen melanoma mole, shown on Figures 1 and 7, respectively.

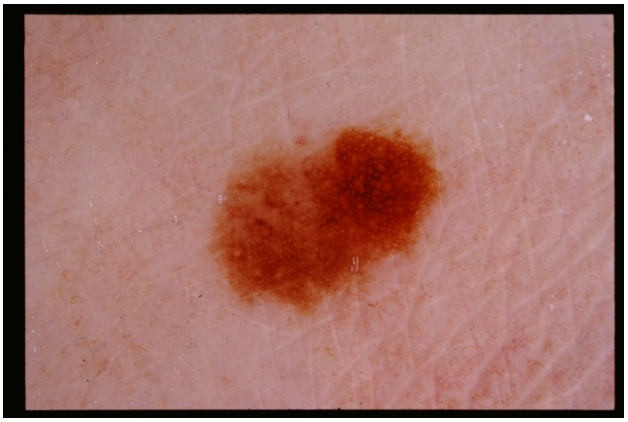

Figure 1. Original image of a randomly chosen non-melanoma mole.

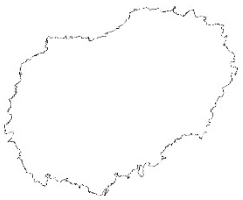

Figure 2. Contour of the mole from the Figure 1 obtained by the Default thresholding algorithm

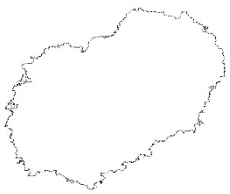

Figure 3. Contour of the mole from the Figure 1 obtained by the Huang thresholding algorithm.

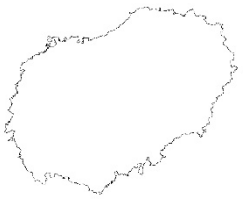

Figure 4. Contour of the mole from the Figure 1 obtained by the Intermodes thresholding algorithm.

Figure 5. Contour of the mole from the Figure 1 obtained by the Minimum thresholding algorithm

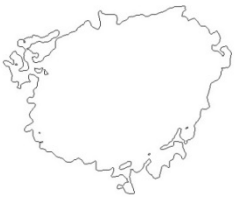

Figure 6. Contour of the mole from the Figure 1 obtained by our MATLAB algorithm

Figure 7. Original image of a randomly chosen melanoma mole.

Figure 8. Contour of the mole from the Figure 7 obtained by the Default thresholding algorithm.

Figure 9. Contour of the mole from the Figure 7 obtained by the Huang thresholding algorithm.

Figure 10. Contour of the mole from the Figure 7 obtained by the Intermodes thresholding algorithm.

Figure 11. Contour of the mole from the Figure 7 obtained by the Minimum thresholding algorithm.

Figure 12. Contour of the mole from the Figure 7 obtained by our MATLAB algorithm.

The distributions of the fractal dimensions of the contours extracted by the Default thresholding algorithm and computed by Harfa, Fraclac, Fractalyse, Fractal Count and Fractal Analysis System, are presented by the histograms given on Figures 13-17. The horizontal axis is for the values of fractal dimension, whilst the vertical is for the number of moles. The histograms themselves show that there is no good differentiation between melanoma and non-melanoma moles. It can be observed that the fractal dimensions of the melanoma and non-melanoma moles belong to overlapping intervals with wide overlapping part.

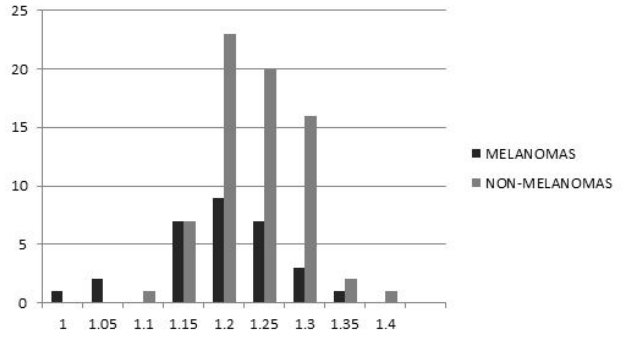

Figure 13. Histogram of the estimated fractal dimensions by Harfa, for outlines obtained by the Default thresholding algorithm.

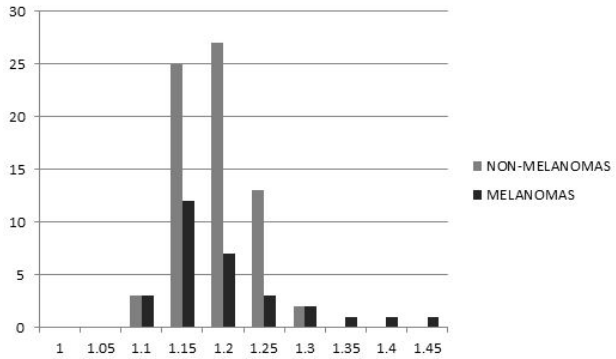

Figure 14. Histogram of the estimated fractal dimensions by FracLac, for contours obtained by the Default thresholding algorithm.

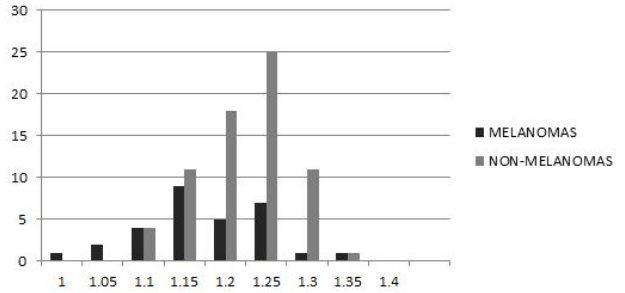

Figure 15. Histogram of the estimated fractal dimensions by Fractalyse, for contours obtained by the Default thresholding algorithm.

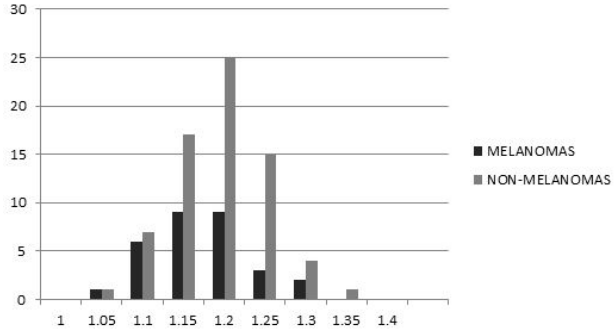

Figure 16. Histogram of the estimated fractal dimensions by Fractal Count, for contours obtained by the Default thresholding algorithm.

Figure 17. Histogram of the estimated fractal dimensions by Fractal Analysis System, for contours obtained by the Default thresholding algorithm.

We additionally computed the means, the standard deviations, the medians, the minimal and the maximal values, and the range of the sets of the fractal dimensions of melanoma and non-melanoma moles in each of the five cases, see Table 1. The table shows that the averages, the medians and the minimal and maximal values of the fractal dimensions of melanoma and non-melanoma moles in all of the 5 cases, have very close values. Taking into consideration the averages of the fractal dimensions of melanoma and non-melanoma moles, FracLac is the only case where the average value of the fractal dimensions of the contours of the melanoma moles is higher than the one of the non-melanoma moles, which coincides with the results that were expected. In all other four cases the opposite happens: the average value of the fractal dimensions of the contours of the melanoma moles is less than the one of the non-melanoma moles. Furthermore, the standard deviations and the range are relatively small, which tells that the accuracy and precision in estimating the fractal dimension should be on a high level.

Having in mind the obtained satisfactory results and the accuracy of FracLac in estimating the fractal dimensions of artificial fractals previously considered ([16]), we decided to make another comparative analysis: to compute by FracLac the fractal dimensions of the contours obtained by the four different ImageJ thresholding algorithms and the MATLAB algorithm. The histogram of the fractal dimensions of the contours obtained by the Default thresholding algorithm is already depicted in Figure 14. Figures 18-21 show the histograms for the results obtained when the other three thresholding algorithms and the MATLAB algorithm are employed.

Table 1. The results for the means, standard deviations, medians, minimal and maximal values and range of the fractal dimensions of the contours extracted by the Default thresholding algorithm of melanoma and non-melanoma moles for five cases: when the fractal dimension is estimated by Harfa, Fractalyse, FracLac, Fractal Count and Fractal Analysis System.

		Average	St. Dev.	Median	Minimal fr. dim.	Maximal fr. dim.	Range
Harfa	Melanoma	1.1722	0.0761	1.1826	0.9848	1.3421	0.3573
	Non-mel.	1.2152	0.0526	1.2144	1.0841	1.3656	0.2815
Fractalyse	Melanoma	1.1572	0.0684	1.1500	1.0130	1.3190	0.3060
	Non-mel.	1.1993	0.0556	1.2055	1.0560	1.3380	0.2820
FracLac	Melanoma	1.1792	0.0788	1.1570	1.0676	1.4270	0.3594
	Non-mel.	1.1650	0.0439	1.1642	1.0739	1.2642	0.1903
Fractal Count	Melanoma	1.1473	0.0631	1.1363	1.0066	1.2740	0.2674
	Non-mel.	1.1712	0.0576	1.1731	1.0428	1.3145	0.2717
Fract. An. Syst.	Melanoma	1.1417	0.0633	1.1362	1.0403	1.2968	0.2565
	Non-mel.	1.1920	0.0559	1.1989	1.0620	1.3102	0.2482

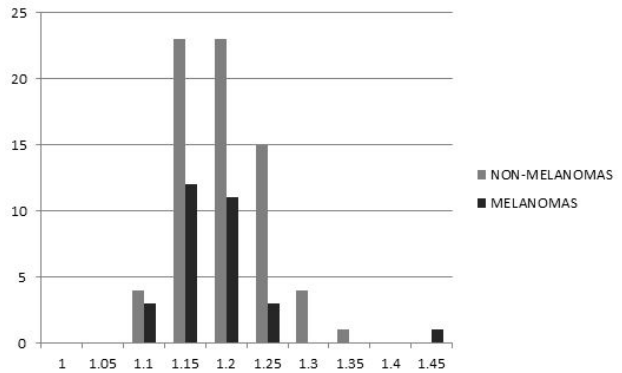

Figure 18. Histogram of the computed fractal dimensions by FracLac, for the contours obtained by the Huang thresholding algorithm.

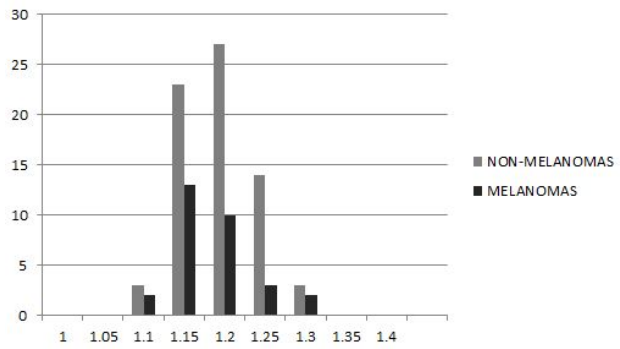

Figure 19. Histogram of the computed fractal dimensions by FracLac, for the contours obtained by the Intermodes thresholding algorithm.

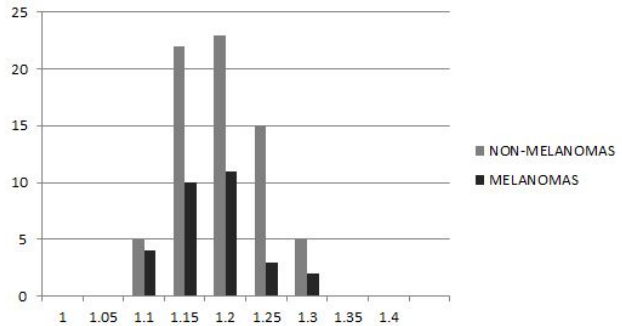

Figure 20. Histogram of the computed fractal dimensions by FracLac, for the contours obtained by the Minimum thresholding algorithm.

Figure 21. Histogram of the computed fractal dimensions by FracLac, for the contours obtained by our MATLAB algorithm.

For the five cases when the fractal dimensions are estimated by FracLac and the contours are obtained by the five thresholding algorithms: Default, Huang, Intermodes, Minimum and our MATLAB, also student's *t*-tests were conducted. We denoted the number of melanoma moles by n_x, $n_x = 30$, and the number of non-melanoma moles by n_y, $n_y = 70$. The means of the fractal dimension of contour-lines of melanoma moles ($\bar{x}$) and non-melanoma moles ($\bar{y}$), the standard deviations of the

fractal dimensions of contour-lines of melanoma moles (σ_x) and non-melanoma moles (σ_y), thresholded by the Default thresholding algorithm, and computed by different software tools, are given in Table 2.

The main question of the research is: "Is it possible to make a distinction between the sets of the fractal dimensions of melanoma and non-melanoma moles? Do they belong to two different sets (clusters)?"

We set the following null hypothesis, H_0: There is no statistical difference between the two sets, the first one consisted of the fractal dimensions of non-melanoma, and the second one consisted of the fractal dimensions of melanoma moles. The alternative hypothesis, H_1 will be: There is a statistical difference between the two sets of moles (two-tailed hypothesis).

To permit a decision between the null hypothesis and the alternative hypothesis, the level of significance α has been chosen to be equal to 0.05 (or 5%). The two-sample *t*-tests are conducted using the R programming language. The obtained results for *t*-value and *p*-value are given in Table 2. With a defined level of significance, *p*-values allow a decision about the rejection or maintenance of a null hypothesis. Since the p-values are greater than the predefined level of significance in all cases (see Table 2), we can conclude that the null hypothesis can not be rejected, which speaking in the statistical language means that the results are not significant. This implies that we can not distinguish two separate sets, one with fractal dimensions of melanoma, and the other with fractal dimensions of non-melanoma moles.

Table 2. Results for verification of the hypothesis related with the fractal dimensions of contour-lines of melanoma and non-melanoma moles, thresholded by the Default, Intermodes, Huang, Minimum and MATLAB thresholding algorithms, computed by FracLac

		Default	Intermodes	Huang	Minimum	MATLAB
	$\bar{x}$	1.1792	1.1611	1.1614	1.1596	1.53210
	σ_x	0.0788	0.0484	0.0631	0.0551	0.01967
	$\bar{y}$	1.1650	1.1669	1.1684	1.1703	1.52459
	σ_y	0.0439	0.0556	0.0507	0.0503	0.01578
	n_x	30	30	30	30	30
	n_y	70	70	70	70	70
H_1: $E(x) \neq E(y)$	*t*-value	-0.91139	0.54753	0.52753	0.89787	1.6466
	p-value	0.368	0.5864	0.6998	0.8132	0.1087
	Comparison	0.368 < 0.05	0.5864 < 0.05	0.6998 < 0.05	0.8132 < 0.05	0.1087 < 0.05
	Is H_0 rejected?	No	No	No	No	No
H_1: $E(x) > E(y)$	*t*-value	0.91139	-0.54753	-0.52753	-0.89787	1.6466
	p-value	0.184	0.7068	0.6998	0.8132	0.05437
	Comparison	0.184 < 0.05	0.7068 < 0.05	0.6998 < 0.05	0.8132 < 0.05	0.05437 < 0.05
	Is H_0 rejected?	No	No	No	No	No
H_1: $E(x) < E(y)$	*t*-value	0.91139	-0.54753	-0.52753	-0.89787	1.6466
	p-value	0.816	0.2932	0.3002	0.1868	0.9456
	Comparison	0.816 < 0.05	0.2932 < 0.05	0.3002 < 0.05	0.1868 < 0.05	0.9456 < 0.05
	Is H_0 rejected?	No	No	No	No	No

In addition, we had examined not just two-tailed alternative hypothesis (any difference), but also the one-tailed alternative hypotheses, where the mathematical expectation of the set of the fractal dimensions of melanoma moles is greater or less then the mathematical expectation of the set of the fractal dimensions of non-melanoma moles. The results are given in Table 2. Again, the *p*-values are greater than the level of significance for all thresholding algorithms; so we can conclude that we can not reject the null hypothesis.

The obtained results lead us to the conclusion that for the sample used in our research, using five different thresholding algorithms for extracting the contour-lines and estimating their fractal dimensions by FracLac software tool, there is no statistical difference between the fractal dimensions of melanoma and non-melanoma moles.

6 Conclusion

As it is noted ([23]), medical images typically suffer from at least one of the following deficiencies: low resolution, high level of noise, low contrast, geometric deformations, presence of imaging artefacts. Highly trained technicians and clinicians could bring these influences to a minimum. Additionally, in recent years there are lot of improvements in hardware, acquisition methods, signal processing techniques and mathematical methods. However, different papers show (see

Section 2) that the fractal dimension depends on the following factors:

- the pixelization of the images,
- the resolution of the images,
- the edge-detection algorithm used,
- the scale at which the object is considered,
- the noise in the images,
- the thresholding algorithm, and
- the estimator used.

In our paper we give additional value to the last two factors, thresholding algorithm and estimator used. Additionally, with statistical means (descriptive statistics and *t*-tests), we showed that there is no statistical difference between the fractal dimensions of melanoma and non-melanoma moles. We would like to emphasize that, in order to make a proper conclusions, a clear distinction between the statistical and clinical significance has to be made. If there is no statistical significance, the results of the clinical significance (or relevance) are not automatically unimportant. One of the reasons can be that the sample size is too small, or the dispersion of the samples is too great. This requires further investigation.

Furthermore, in this occasion we would like to highlight the struggle that occurs when well defined mathematical theory should be put in use. When the precisely, asymptotically defined scalar, as the fractal dimension is, should characterize images dependent on many factors and limitations, many ambiguities happen. Especially when that estimated number is needed to be precise and accurate. Deeper understanding of all positive and negative sides of the instruments of the fractal analysis, both from theoretical and practical aspects, is of crucial importance. Although in the papers considered in the Section 2, the authors give suggestions for the improvement of particular steps of the fractal analysis, there is a lot of randomness, arbitrariness, relativeness, beneficial and non-beneficial coincidences, that according to our investigations, will always yield to non-reliable results in practical applications.

Acknowledgment

The authors would like to thank to Zoran Ivanovski, Carlo Ciulla, Aleksandar Karadimce and Ljubinka Gjergjeska, for their help in our work on this paper.

References:

[1] E. Claridge, P.N. Hall, M. Keefe, J.P. Allen, Shape Analysis for Classification of Malignant Melanoma, *JBE* 14 (3), 1992, pp. 229-234.

[2] K. Klein, T. Maier, V.C. Hirschfeld-Warneken, J.P. Spatz, Marker-Free Phenotyping of Tumor Cells by Fractal Analysis of Reflection Interference Contrast Microscopy Images, *NL, ACS Publications, American Chemical Society*, dx.doi.org/10.1021/nl4030402 | Nano Lett. 2013, 13, 2013, pp. 5474-5479.

[3] P. Y. Kim, K.M. Iftekharuddin, P.G. Davey, M. Toth, A. Garas, G. Hollo, E.A. Essock, Novel Fractal Feature-Based Multiclass Glaucoma Detection and Progression Prediction, *BHI, IEEE Journal of*, 17, no.2, March 2013, pp. 269-276, doi: 10.1109/TITB.2012.2218661.

[4] M. Mastrolonardo, E. Conte, J.P. Zbilut, 2006. A fractal analysis of skin pigmented lesions using the novel tool of the variogram technique, CSF, 28, 2006, pp. 1119-1135.

[5] A. Piantanelli, P. Maponi, L. Scalise, S. Serresi, A. Cialabrini, A. Basso, Fractal characterisation of boundary irregularity in skin pigmented lesions, MBEC. Jul; 43 (4), 2005, pp. 436-42.

[6] E. Zagrouba, W. Barhoumi, A preliminary approach for the automated recognition of malignant melanoma, *IAS*, 23, 2004, pp. 121-135.

[7] R. Dobrescu, M. Dobrescu, S. Mocanu and D. Popescu, Medical Images Classification for Skin Cancer Diagnosis Based on Combined Texture and Fractal Analysis, *WSEAS Transactions on Biology and Biomedicine*, 7, no. 3, 2010. pp. 223-232.

[8] R. Lopes, N. Betrouni, Fractal and multifractal analysis: A review, Medical Image Analysis, 13, 2009, pp. 634-649.

[9] S. Criscuoli, M.P. Ras, I. Ermolli and M. Centrone, On the reliability of the fractal dimension measure of solar magnetic features and on its variation with solar activity, *AA*, 461, 2007, pp. 331-338, DOI: 10.1051/0004-6361:20065951.

[10] H. Ahammer, T.T.J. DeVaney, The influence of edge detection algorithms on the estimation of the fractal dimension of binary digital images, *C*, 14(1), 2004, pp. 183-8.

[11] B. Braverman, M. Tambasco, Scale-Specific Multifractal Medical Image Analysis, CMMM, 2013, *Hindawi Publishing Corporation*, Article ID 262931, 2013, 11 pages, http://dx.doi.org/10.1155/2013/262931.

[12] A. R. Martin, N. Sabathiel, H. Ahammer, Noise dependency of algorithms for calculating fractal dimensions in digital images, *CSF*, 78, 2015, pp. 39-46.

[13] B. Mandelbrot, *The Fractal Geometry of Nature*, W. H. Freeman, San Francisco, 1982.

[14] K. J. Falconer, Fractal Geometry. *Mathematical foundations and Applications*, John Wiley and Sons, England, 1990

[15] M. F. Barnsley, *Fractals everywhere*, Academic Press, USA, 1988.
[16] E. Hadzieva, D. C. Bogatinoska, Lj. Gjergjeska, M. Shuminoska, R. Petreski, Review of the Software Tools for Estimating the Fractal Dimension, S. Loshkovska, S. Koceski (Editors): *ICT Innovations* 2015, Web Proceedings, ISSN 1857-7288, 2015, p. 201-211.
[17] E. Hadzieva, D. C. Bogatinoska, R. Petroski, M. Shuminoska, Lj. Gjergjeska, A. Karadimce, V. Trajkova, Is the Fractal Dimension of Contour-lines a reliable Tool For Classification of Medical Images?, accepted for publishing for MATEC Web of Conferences.
[18] O. Zmeškal, M. Vesely, M. Nezadal, M. Buchniček, Fractal Analysis of Image Structures, HarFA - Harmonic and Fractal Image Analysis, 2001, pp. 3-5.
[19] M. E. Celebi, A. Aslandogan, W. V. Stoecker, Unsupervised Border Detection in Dermoscopy Images, *SRT*, 13(4), 2007, pp. 454–462.
[20] M. E. Celebi, H. Kingravi, H. Iyatomi, A. Aslandogan, W. V. Stoecker, R. H. Moss, Border Detection in Dermoscopy Images Using Statistical Region Merging, *SRT*, 14(3), 2008, pp. 347–353.
[21] M. E. Celebi, H. Iyatomi, G. Schaefer, W. V. Stoecker, Lesion Border Detection in Dermoscopy Images, *CMIG*, 33(2), 2009, pp. 148–153.
[22] M. E. Celebi, Q. Wen, S. Hwang, H. Iyatomi, G. Schaefer, Lesion Border Detection in Dermoscopy Images Using Ensembles of Thresholding Methods, Skin Research and Technology, 19(1), 2013, pp. e252–258.
[23] S. Angenent, E. Pichon, A. Tannenbaum, Mathematical Methods in Medical Image Processing, *BAMS*. 43, 2006, pp. 365-396.
[24] https://www.melanoma.org/understand-melanoma/diagnosing-melanoma/detection-screening/abcdes-melanoma
[25] http://www.fch.vutbr.cz/lectures/imagesci/
[26] http://rsb.info.nih.gov/ij/plugins/fraclac
[27] http://www.fractalyse.org/
[28] http://www.pvv.org/~perchrh/imagej/fractal.html
[29] http://cse.naro.affrc.go.jp/sasaki/fractal/fractal-e.html